Nuclear Physics B84 (1975) 375–396. North-Holland Publishing Company

BETHE-SALPETER EQUATION FOR $J = 0$ NUCLEON-NUCLEON SCATTERING WITH ONE-BOSON EXCHANGE

J. FLEISCHER *
Department of Theoretical Physics, University of Bielefeld, Germany

J.A. TJON
Institute for Theoretical Physics, University of Utrecht, The Netherlands

Received 8 July 1974

Abstract: The Bethe-Salpeter equation is solved numerically for the $J = 0$ nucleon-nucleon phase shifts by iteration and summation of the perturbation series with Padé approximants. As kernel a superposition of π-, η-, ϵ-, δ-, ρ- and ω-exchange is used, taking completely into account the complications due to the various spin- and positive and negative energy-states. Considerable deviations of our phase shifts from the ones as calculated by means of the Blankenbecler-Sugar equation are found. A reasonable reproduction of the $^1S_0$ and $^3P_0$ phase shifts in the framework of the Bethe-Salpeter equation is obtained by introducing a large ωNN coupling.

1. Introduction

Nucleon-nucleon scattering has been described successfully in terms of the Schrödinger equation [1, 2] with the potential consisting of a central part, spin-orbit, tensor and spin-spin couplings. If one wants to take into account quantum field theory and relativistic effects, however, one has to use the Bethe-Salpeter equation (BSE). Fortes and Jackson [3] discussed the BSE for scalar nucleons with scalar meson exchange. They found considerable effects in comparison with the Blankenbecler-Sugar (BBS) and Lippmann-Schwinger reductions of the BSE. These were particularly large when cancellations between attractive and repulsive terms in the interaction occurred.

In view of this and also since there are large matrix elements for pseudoscalar exchange between positive and negative energy states it seems to be an important task to take into account the full BSE and investigate its consequences for the NN phase shifts. Because of the coupling of the various positive and negative energy states and the different spin states, the BSE is a very complex multichannel problem:

* Supported by the Deutsche Forschungsgemeinschaft.

for total angular momentum $J = 0$ it consists of four and for $J > 0$ of eight coupled singular integral equations in two variables. For $J = 0$ and the simplest kernels (pseudoscalar-, scalar- and "photon"-exchange) mathematical properties of the BSE have been studied and qualitative effects elaborated [4, 5]. In this work we take into account the complete kernels of one-boson exchanges for the experimentally known bosons. A cutoff is clearly needed. For computational reasons we presently confine ourselves to $J = 0$ as well.

In the last few years various investigations of NN scattering have been made on the basis of the BBS type of approximation to the BSE [6, 7, 8]. It is the purpose of the present work to study what effects the full BSE yields compared to its BBS approximation. We did not try to obtain new insight about possible forms of the "potential", like e.g. the two-pion exchange part. Neither did we perform a least square fit to the experimental data by changing coupling constants and exchanged masses. We did, however, try to find a fair reproduction of the phase shifts in the framework of the BSE.

To point out some of our technical means: the analytic calculation of the kernels goes back to the work of Kubis [9] who generalized the helicity formalism of Goldberger et al. [10]. This procedure has been automated in ref. [11] by means of the formulae manipulating language REDUCE [12]. Numerical solutions of the BSE have been obtained by iterating the K-matrix equation and summing the perturbation series by means of Padé approximants. It can be shown that the Padé approximants converge once a cutoff is introduced in the BSE. It has also been tested numerically by Gammel et al. [5] that this procedure is equivalent to matrix inversion. Beyond that it seems to be the only feasible way because matrix inversion works much too slow.

2. The Bethe-Salpeter equation and the one-boson exchange kernels

The BSE in ladder approximation is shown schematically in fig. 1, where we have chosen the following kinematics:

$$p_1 = (E + p_0, \boldsymbol{p}) , \qquad p_1' = (E + p_0', \boldsymbol{p}') ,$$

$$p_2 = (E - p_0, -\boldsymbol{p}) , \qquad p_2' = (E - p_0', -\boldsymbol{p}') ,$$

$$q_1 = (E + q_0, \boldsymbol{q}) , \qquad E^2 = \tfrac{1}{4} s ,$$

$$q_2 = (E - q_0, -\boldsymbol{q}) . \tag{2.1}$$

For on-mass-shell scattering the relative energies p_0 and p_0' are set equal to zero.

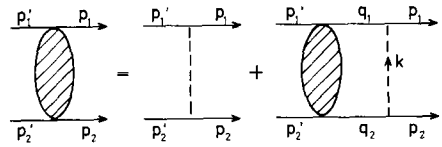

Fig. 1. Graphical representation of the BSE.

The equation reads

$$\phi = \sum_B \frac{V_B^{(1)} V_B^{(2)}}{(p_0 - p_0')^2 - (\boldsymbol{p} - \boldsymbol{p}')^2 - \mu_B^2}$$
$$- \frac{i}{4\pi^3} \int \mathrm{d}q_0 \, \mathrm{d}^3 q \sum_B \frac{V_B^{(1)} V_B^{(2)}}{(p_0 - q_0)^2 - (\boldsymbol{p} - \boldsymbol{q})^2 - \mu_B^2}$$
$$\times \frac{(E + q_0)\gamma_0^{(1)} - \boldsymbol{q} \cdot \boldsymbol{\gamma}^{(1)} + m}{(E + q_0)^2 - E(q)^2} \; \frac{(E - q_0)\gamma_0^{(2)} + \boldsymbol{q} \cdot \boldsymbol{\gamma}^{(2)} + m}{(E - q_0)^2 - E(q)^2} \, \phi \,, \tag{2.2}$$

where $E(q) = \sqrt{m^2 + q^2}$ (m is the nucleon mass) and the superscripts refer to particle 1 and 2. The Σ_B extends over the exchanged bosons (μ_B are the boson masses). We consider a superposition of π-, η-, ϵ-, δ-, ρ- and ω-exchange. According to our notation the coupling constants are part of the vertex operators.

The coupling of bosons to nucleons is described by the following Lagrangians [13]:

$$\mathcal{L} = ig\bar{\psi}\gamma_5 \boldsymbol{\tau}\psi \cdot \boldsymbol{\phi} \,,$$
$$\mathcal{L} = g\bar{\psi}\psi\phi \,,$$
$$\mathcal{L} = g^{\mathrm{V}}\bar{\psi}\gamma_\mu \boldsymbol{\tau}\psi \cdot \boldsymbol{\phi}^\mu - i\frac{g^{\mathrm{T}}}{4m}\bar{\psi}\sigma_{\mu\nu}\boldsymbol{\tau}\psi \cdot (\partial^\mu \boldsymbol{\phi}^\nu - \partial^\nu \boldsymbol{\phi}^\mu) \,, \tag{2.3}$$

for pseudoscalar, scalar and vector bosons, respectively. Here ψ and ϕ denote the nucleon and boson fields.

Accordingly the vertex operators read:

$$V^{(1)} V^{(2)} = \frac{g^2}{4\pi} \gamma_5^{(1)} \gamma_5^{(2)} \tag{2.4}$$

for pseudoscalar exchange and

$$V^{(1)} V^{(2)} = -\frac{g^2}{4\pi} 1^{(1)} 1^{(2)} \tag{2.5}$$

for scalar exchange. For vector exchange we have with $k = p_1 - q_1$ (see fig. 1):

$$V^{(1)} V^{(2)} = \frac{1}{4\pi}\left[g^{\mathrm{V}}\gamma_\mu^{(1)} - \frac{g^{\mathrm{T}}}{2m}\sigma_{\mu\lambda}^{(1)} k^\lambda\right]\left(-g^{\mu\nu} + \frac{k^\mu k^\nu}{\mu_B^2}\right)\left[g^{\mathrm{V}}\gamma_\nu^{(2)} + \frac{g^{\mathrm{T}}}{2m}\sigma_{\nu\kappa}^{(2)} k^\kappa\right], \tag{2.6}$$

which can be reduced to

$$V^{(1)}\,V^{(2)} = \frac{g^{V^2}}{4\pi}\left\{-\gamma_\mu^{(1)}\cdot\gamma^{\mu(2)} + \frac{1}{\mu_B^2}\,\bar{k}^{(1)}\cdot\bar{k}^{(2)}\right\}$$

$$-\frac{g^{T^2}}{4\pi}\,\frac{1}{4m^2}\,\{\bar{k}^{(1)}\gamma_\mu^{(1)}\cdot\gamma^{\mu(2)}\bar{k}^{(2)} - k^2 1^{(1)}\cdot 1^{(2)}\}$$

$$+\frac{g^V g^T}{4\pi}\,\frac{1}{2m}\,\{\gamma_\mu^{(1)}\bar{k}^{(1)}\cdot\gamma^{\mu(2)} - \gamma_\mu^{(1)}\cdot\gamma^{\mu(2)}\bar{k}^{(2)} + \bar{k}^{(1)}\cdot 1^{(2)} - 1^{(1)}\cdot\bar{k}^{(2)}\}. \quad (2.7)$$

Here $1^{(i)}$ $(i = 1,2)$ stand for 4×4 unity matrices.

The partial wave projection of the BSE has been described extensively in refs. [5, 9, 11]. For $J = 0$ four intermediate states couple. These are

$$^1S_0^+\,,\ ^1S_0^-\,,\ ^3P_0^e\,,\ ^3P_0^o\,,$$

$$^3P_0^+\,,\ ^3P_0^-\,,\ ^1S_0^e\,,\ ^1S_0^o\,, \quad (2.8)$$

for the $^1S_0$ and $^3P_0$ partial waves, respectively. The upper r.h. index refers to the "energy-spin" [5]. In the following these states will be labelled 1 through 4, using greek letters for the indices. Latin indices will be used for a labelling from 1 through 3. The coupled integral equations read:

$$\phi(p, p_0, \alpha) = G(p, p_0, \alpha; \hat{p}, 0, 1)$$

$$-\frac{i}{2\pi^2}\int dq\, d_0 \sum_{\beta,\gamma} G(p, p_0, \alpha; q, q_0, \beta)\, S(q, q_0, \beta, \gamma)\phi(q, q_0, \gamma)\,, \quad (2.9)$$

where $\hat{p} = \sqrt{E^2 - m^2}$ is the on-shell c.m. momentum. The desired on-shell transition element is $\phi(\hat{p}, 0, 1)$. The two-nucleon propagator S is independent of spin indices [5]:

$$S = \begin{pmatrix} S_{++} & 0 & & 0 \\ 0 & S_{--} & & \\ & & S_{ee} & S_{eo} \\ 0 & & S_{oe} & S_{oo} \end{pmatrix}, \quad (2.10)$$

where

$$S_{++} = \frac{1}{(E - E(q) + i\epsilon)^2 - q_0^2}\,,$$

$$S_{--} = \frac{1}{(E + E(q) - i\epsilon)^2 - q_0^2} ,$$

$$S_{ee} = S_{oo} = \frac{1}{2E}\left[\frac{E - E(q)}{(E - E(q) + i\epsilon)^2 - q_0^2} + \frac{E + E(q)}{(E + E(q) - i\epsilon)^2 - q_0^2}\right],$$

$$S_{eo} = S_{oe} = -\frac{q_0}{2E}\left[\frac{1}{(E - E(q) + i\epsilon)^2 - q_0^2} - \frac{1}{(E + E(q) - i\epsilon)^2 - q_0^2}\right]. \tag{2.11}$$

The explicit expressions for the kernels $G(p, p_0, \alpha; q, q_0, \beta)$ corresponding to the vertex functions (2.4), (2.5) and (2.7) were calculated by means of the formulae manipulating language REDUCE [12]. Ref. [11] gives a description of the code. The elements are listed in appendix A. In the following we explore some of their symmetry properties.

Due to T invariance, G is symmetric under transposition and simultaneous exchange of (p, p_0) and (q, q_0) which amounts to an exchange of initial and final states. Furthermore the following equalities hold:

$$G(2,1) = G(1,2), \qquad G(2,2) = G(1,1) ,$$
$$G(2,3) = -G(1,3), \qquad G(2,4) = -G(1,4). \tag{2.12}$$

These relations have been found by explicitely calculating all elements and can be understood from CP invariance. Due to (2.12) the kernel simplifies considerably in the following new basis:

$$\langle'1'| = \frac{\langle 1| + \langle 2|}{\sqrt{2}} , \qquad \langle'2'| = \frac{\langle 1| - \langle 2|}{\sqrt{2}} , \tag{2.13}$$

the third and fourth state unchanged. The first row and column of G vanish completely in this basis, except for the (1,1) element. In particular the transformed upper l.h. 2×2 matrix reads in terms of the original elements:

$$\begin{bmatrix} G(1,1) + G(1,2) & 0 \\ 0 & G(1,1) - G(1,2) \end{bmatrix} . \tag{2.14}$$

As the (1,1) and (1,2) elements differ only in the sign of the terms proportional to even powers (0 and 2) of $E(q)$ while the ones with odd powers (1 and 3) are the same (see appendix A), the elements of matrix (2.14) contain only even or odd powers of $E(q)$. This is so for the (3,3) and (4,4) elements as well. We do not, however, assume that there is a deep reason behind this amazing rule.

In the new basis the two-nucleon propagator does not diagonalize anymore. Therefore the breakup of the kernel into two submatrices does not imply a decoupling of the integral equations and the only advantage of basis (2.13) is a greater transparency of the kernel.

Finally we have:

$$G(3,4) = g(p)\, G(2,4)\,. \tag{2.15}$$

This relation is only relevant for vector exchange (for pseudoscalar and scalar exchange both elements vanish), where $g(p)$ differs for the mixed term ($\sim g^{\mathrm{V}} g^{\mathrm{T}}$) from the pure vector and tensor couplings. Putting the nucleon mass $m = 1$ in the following, it is $g(p) = \sqrt{2}\, p$ for the pure coupling terms and $g(p) = -\sqrt{2}/p$ for the mixed terms.

As a consequence of the above properties there are essentially only 6 different matrix elements for each kernel.

Due to the singular behaviour of the kernels for pseudoscalar as well as for scalar exchange [14] and particularly for vector exchange we have to introduce a cutoff at high momenta. This is done by inserting a "form-factor".

$$F(t) = \frac{-\Lambda^2}{t - \Lambda^2} \tag{2.16}$$

at the meson-nucleon vertices, where Λ is a cutoff mass. As in ref. [7], Λ is taken the same for all exchanged bosons. For the partial waves the introduction of the above formfactor results in subtracting the Q_1 functions.

3. Method of solution for the Bethe-Salpeter equation

The equal masses of the two nucleons (particle 1 and 2) imply some symmetry properties of the Bethe-Salpeter equation in the relative energy which allow to formulate even the Wick rotated equation totally in terms of real quantities. Clearly the diagonal elements of the two-nucleon propagator are even in the relative energy q_0, while the off-diagonal elements are odd (see (2.10)). Concerning the kernel, the basis states in the BSE are chosen such [9] that the elements (a, b) and $(4,4)$ are even and $(a,4)$ and $(4,a)$ are odd in the relative energies ($a = 1,2,3$). Hence $\phi(p,p_0,a)$ is even and $\phi(p,p_0,4)$ is odd in the relative energy p_0. Accordingly we can at first change the range of the q_0 integration. Introducing

$$\begin{aligned} G_+(p,p_0,\alpha;q,q_0,\beta) &= \tfrac{1}{2}\,[G(p,p_0,\alpha;q,q_0,\beta) + G(p,p_0,\alpha;q,-q_0,\beta)]\,, \\ G_-(p,p_0,\alpha;q,q_0,\beta) &= \tfrac{1}{2}\,[G(p,p_0,\alpha;q,q_0,\beta) - G(p,p_0,\alpha;q,-q_0,\beta)]\,, \end{aligned} \tag{3.1}$$

eq. (2.9) can be written as

$$\begin{aligned} \phi(p,p_0,\alpha) = {} & G(p,p_0,\alpha;\hat{p},0,1) - \frac{i}{\pi^2} \int_0^\infty \mathrm{d}q\, \mathrm{d}q_0 \sum_{b,c} \{\, G_+(p,p_0,\alpha;q,q_0,b) \\ & \times S(q,q_0,b,c)\phi(q,q_0,c) + G_+(p,p_0,\alpha;q,q_0,b) S(q,q_0,b,4)\phi(q,q_0,4) \\ & + G_-(p,p_0,\alpha;q,q_0,4) S(q,q_0,4,c)\phi(q,q_0,c) + G_-(p,p_0,\alpha;q,q_0,4) S(q,q_0,4,4)\phi(q,q_0,4)\,\}, \end{aligned} \tag{3.2}$$

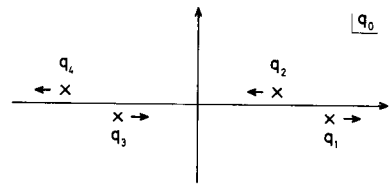

Fig. 2. Poles of the two-nucleon propagator in the q_0 plane.

where the symmetry properties of S and ϕ determine the choice of G_+ and G_-.

In this work we confine ourselves to energies below the one-pion production threshold. Hence the singularity properties of the BSE are completely due to two particle unitarity. Fig. 2 shows the poles of the two-nucleon propagator in the q_0 plane, which are

$$\begin{aligned} q_1 &= E + E(q) - i\epsilon\,, & q_2 &= E - E(q) + i\epsilon\,, \\ q_3 &= -E + E(q) - i\epsilon\,, & q_4 &= -E - E(q) + i\epsilon\,. \end{aligned} \tag{3.3}$$

For $q = \hat{p}$ the poles q_2 and q_3 pinch the q_0 path at $q_0 = 0$. The principal value in the q-integration gives us the tangent of the phase shift (K-matrix):

$$\operatorname{tg}\delta = \frac{E}{2\hat{p}}\,\phi(\hat{p},0,1)\,. \tag{3.4}$$

This principal value integration is performed as follows: the integral in eq. (3.2) reads in an obvious abbreviation:

$$I_\alpha = -\frac{i}{\pi^2}\int_0^\infty \mathrm{d}q \int_0^\infty \mathrm{d}q_0 \sum_{\beta,\gamma} K(p,p_0,\alpha;q,q_0,\beta)S(q,q_0,\beta,\gamma)\phi(q,q_0,\gamma)\,. \tag{3.5}$$

To split off the scalar propagator we write

$$I_\alpha = -\frac{i}{\pi^2}\int_0^\infty \mathrm{d}q \int_0^\infty \mathrm{d}q_0\, A_\alpha(p,p_0;q,q_0)f(q,q_0)\,, \tag{3.6}$$

with

$$A_\alpha = \sum_{\beta,\gamma} K(p,p_0,\alpha;q,q_0,\beta)\frac{S(q,q_0,\beta,\gamma)}{f(q,q_0)}\,\phi(q,q_0,\gamma)\,, \tag{3.7}$$

$$f(q,q_0) = \frac{q}{E(q)}\,S_{++}(q,q_0)S_{--}(q,q_0) = \frac{q}{E(q)}\prod_{i=1}^{4}\frac{1}{q_0 - q_i}\,. \tag{3.8}$$

The functions A_α are smooth in (q,q_0) and the singularities are contained in $f(q,q_0)$ only. We now perform the following subtraction:

$$I_\alpha = -\frac{i}{\pi^2} \int_0^\infty \mathrm{d}q \int_0^\infty \mathrm{d}q_0 \{A_\alpha(p,p_0;q,q_0) - A_\alpha(p,p_0;\hat{p},0)\} f(q,q_0)$$
$$+ \text{subt}\, A_\alpha(p,p_0;\hat{p},0)\,, \tag{3.9}$$

with

$$\text{subt} = -\frac{i}{\pi^2}\, \mathrm{P} \int_0^\infty \mathrm{d}q \int_0^\infty \mathrm{d}q_0 f(q,q_0)\,, \tag{3.10}$$

which can be evaluated analytically to give

$$\text{subt} = -\frac{1}{4\pi E^2} \ln \hat{p}\,. \tag{3.11}$$

On the basis of this subtraction procedure we perform the iteration of the BSE. In view of the fact that the BSE with the cutoff as introduced in sect. 2 can be reduced to a non-singular integral equation (see ref. [15]), we know that the resulting T-matrix is mesomorphic in the coupling constant. As a consequence, due to a conjecture of Chisholm [16], proven later on rigorously by Nuttall and Baker [17], the Padé approximants for the T-matrix converge to the solution of the BSE. Using this fact the perturbation series was summed by means of Padé approximants. The rate of convergence turns out to be fast enough for practical purposes.

4. Wick rotation

The integral in (3.9) can be computed by means of the Wick rotation, which results in a 90° rotation of the q_0 integration path, changing q_0 into iq_4. A contribution from the pole q_2 (see (3.3) and fig. 2) is picked up in performing this rotation and the BSE reads:

$$\phi(p,ip_4,\alpha) = G(p,ip_4,\alpha;\hat{p},0,1)$$
$$+\frac{1}{\pi^2} \int_0^\infty \mathrm{d}q \int_0^\infty \mathrm{d}q_4 \{A_\alpha(p,ip_4;q,iq_4) - A_\alpha(p,ip_4;\hat{p},0)\} f(q,iq_4)$$
$$+\frac{1}{\pi} \int_0^{\hat{p}} \mathrm{d}q \{A_\alpha(p,ip_4;q,E-E(q)) - A_\alpha(p,ip_4;\hat{p},0)\} f_\mathrm{R}(q)$$
$$+ \text{subt}\, A_\alpha(p,ip_4;\hat{p},0)\,, \tag{4.1}$$

where $f_\mathrm{R}(q)$ is twice the residue of $f(q,q_0)$ at the pole q_2:

$$f_\mathrm{R}(q) = \frac{q}{4E(q)^2 E} \frac{1}{E(q)-E}\,. \tag{4.2}$$

The value of $\bar{S} = S/f(q,q_0)$ at the same pole enters the single integral. It is given by

$$\bar{S}_R(q) = \frac{S_R(q)}{f_R(q)} , \tag{4.3}$$

where $S_R(q)$ is twice the residue of S at the pole q_2:

$$S_R(q,E-E(q),1,1) = \frac{1}{E(q)-E} ,$$

$$S_R(q,E-E(q),2,2) = 0 ,$$

$$S_R(q,E-E(q),3,3) = S_R(q,E-E(q),4,4) = -\frac{1}{2E} ,$$

$$S_R(q,E-E(q),3,4) = S_R(q,E-E(q),4,3) = \frac{1}{2E} . \tag{4.4}$$

The appearance of $\phi(q,E-E(q),\gamma)$ through the single integral of (4.1) and the definition (3.7) requires the auxiliary equation

$$\begin{aligned}\phi(p,E-E(p),\alpha) &= G(p,E-E(p),\alpha;\hat{p},0,1)\\ &+\frac{1}{\pi^2}\int_0^\infty dq \int_0^\infty dq_4 \{A_\alpha(p,E-E(p);q,iq_4) - A_\alpha(p,E-E(p);\hat{p},0\} f(q,iq_4)\\ &+\frac{1}{\pi}\int_0^{\hat{p}} dq \{A_\alpha(p,E-E(p);q,E-E(q)) - A_\alpha(p,E-E(p);\hat{p},0)\} f_R(q)\\ &+ \text{subt}\, A_\alpha(p,E-E(p);\hat{p},0) .\end{aligned} \tag{4.5}$$

(4.1) and (4.5) are now a complete set of integral equations which has to be solved for $\phi(\hat{p},0,1)$. They still contain complex quantities which shall be eliminated in the following.

Due to their symmetry properties, the diagonal elements of $S(q,iq_4,\alpha,\beta)$ are real, while the off-diagonal elements are purely imaginary. Similarly $\phi(p,ip_4,a)$ is real and $\phi(p,ip_4,4)$ is purely imaginary. Therefore we split off factors i according to

$$\phi(p,ip_4,4) := \frac{1}{i}\,\phi(p,ip_4,4) ,$$

$$S(q,iq_4,3,4) := i\,S(q,iq_4,3,4) ,$$

$$S(q,iq_4,4,3) := \frac{1}{i}\,S(q,iq_4,4,3) . \tag{4.6}$$

The resulting K's are then:

$$K(p,ip_4,a;q,iq_4,b) = G_+(p,ip_4,a;q,iq_4,b) ,$$

$$K(p,ip_4,a;q,iq_4,4) = \frac{1}{i} G_-(p,ip_4,a;q,iq_4,4)\,,$$

$$K(p,ip_4,4;q,iq_4,b) = i\,G_+(p,ip_4,4;q,iq_4,b)\,,$$

$$K(p,ip_4,4;q,iq_4,4) = G_-(p,ip_4,4;q,iq_4,4)\,; \tag{4.7}$$

$$K(p,ip_4,a;q,E-E(q),b) = \mathrm{Re}\, G(p,ip_4,a;q,E-E(q),b)\,,$$

$$K(p,ip_4,a;q,E-E(q),4) = \mathrm{Re}\, G(p,ip_4,a;q,E-E(q),4)\,,$$

$$K(p,ip_4,4;q,E-E(q),b) = -\mathrm{Im}\, G(p,ip_4,4;q,E-E(q),b)\,,$$

$$K(p,ip_4,4;q,E-E(q),4) = -\mathrm{Im}\, G(p,ip_4,4;q,E-E(q),4)\,; \tag{4.8}$$

$$K(p,E-E(p),a;q,iq_4,b) = \mathrm{Re}\, G(p,E-E(p),a;q,iq_4,b)\,,$$

$$K(p,E-E(p),a;q,iq_4,4) = \mathrm{Im}\, G(p,E-E(p),a;q,iq_4,4)\,,$$

$$K(p,E-E(p),4;q,iq_4,b) = \mathrm{Re}\, G(p,E-E(p),4;q,iq_4,b)\,,$$

$$K(p,E-E(p),4;q,iq_4,4) = \mathrm{Im}\, G(p,E-E(p),4;q,iq_4,4)\,; \tag{4.9}$$

$$K(p,E-E(p),a;q,E-E(q),b) = G_+(p,E-E(p),a;q,E-E(q),b)\,,$$

$$K(p,E-E(p),a;q,E-E(q),4) = G_-(p,E-E(p),a;q,E-E(q),4)\,,$$

$$K(p,E-E(p),4;q,E-E(q),b) = G_+(p,E-E(p),4;q,E-E(q),b)\,,$$

$$K(p,E-E(p),4;q,E-E(q),4) = G_-(p,E-E(p),4;q,E-E(q),4)\,. \tag{4.10}$$

These are all real, i.e. splitting off factors i properly renders eqs. (4.1) and (4.5) real. Observe that due to (4.6) S_{34} and S_{43} have now opposite sign. The non-vanishing elements $(a,4)$ and $(4,a)$ in our kernel make the above list of K's slightly more elaborate than in earlier work on the Bethe-Salpeter equation [5].

5. Numerical integration procedure

We now have to find an integration procedure adequate for the numerical integration of eqs. (4.1) and (4.5). Due to the subtraction the one-dimensional integrals have become completely smooth and can be treated numerically by the use of Gaussian integration. In the two-dimensional integrations there is still a single pole

left at the point $q = \hat{p}$, $q_4 = 0$. Near this point the integrand can be written as

$$F(q,q_4) = \frac{(q-\hat{p})A_1 + q_4 A_2}{q_4^2 + (E-E(q))^2}\,, \tag{5.1}$$

where A_1 and A_2 are smooth functions of q and q_4. To see the type of singularity, we integrate near this point of a given q over q_4. One finds a logarithmic singularity in q. Hence for (q,q_4) near $(\hat{p},0)$ one has

$$\int F(q,q_4)\,\mathrm{d}q_4 \sim \ln|q-\hat{p}|\,.$$

This is of course an integrable singularity, but for numerical purpose still rather bad. To get rid of this we split the integral over q between 0 and ∞ into two pieces namely

$$\text{(a) } 0 \leqslant q \leqslant 2\hat{p} \quad \text{and} \quad \text{(b) } q \geqslant 2\hat{p}\,. \tag{5.3}$$

The first integral $\int_0^{2\hat{p}} \mathrm{d}q$ is done by a change of variable. Instead of q we use the variable x:

$$x = \hat{p} - \{|q-\hat{p}|\hat{p}\}^{\frac{1}{2}} \quad \text{for } 0 \leqslant q \leqslant \hat{p}\,,$$

$$x = \hat{p} + \{|q-\hat{p}|\hat{p}\}^{\frac{1}{2}} \quad \text{for } \hat{p} \leqslant q \leqslant 2\hat{p}\,. \tag{5.4}$$

The region of x is then $x \in [0,2\hat{p}]$ and the inverse transformation reads:

$$q = \hat{p} - (x-\hat{p})^2/\hat{p} \quad \text{for } 0 \leqslant x \leqslant \hat{p}\,,$$

$$q = \hat{p} + (x-\hat{p})^2/\hat{p} \quad \text{for } \hat{p} \leqslant x \leqslant 2\hat{p}\,. \tag{5.5}$$

Since

$$\frac{\mathrm{d}q}{\mathrm{d}x} = 2\,\frac{|x-\hat{p}|}{\hat{p}}\,, \tag{5.6}$$

we get

$$\int_0^{2\hat{p}} \mathrm{d}q = 2\int_0^{2\hat{p}} \mathrm{d}x\,\frac{|x-\hat{p}|}{\hat{p}}\,. \tag{5.7}$$

Hence the singularity has become much smoother, namely of the type

$$|x-\hat{p}|\ln|x-\hat{p}| \quad \text{for } x \text{ near } \hat{p}\,, \tag{5.8}$$

which can be handled numerically in a more accurate way by simple use of gaussian points. In order to get a more accurate result an even number of points should be taken, since then one has automatically a symmetric integration around the point of singularity.

The second integral $\int_{2\hat{p}}^{\infty} \mathrm{d}q$ is done by the simple mapping

$$q = C_p \frac{x}{1-x} + 2\hat{p}\,, \qquad \text{with } x \in [0,1]\,. \tag{5.9}$$

Also the q_4 integration is done by

$$q_4 = C_{p_4} \frac{x^2}{1-x}\,, \qquad \text{with } x \in [0,1]\,. \tag{5.10}$$

For x a N-point Gaussian distribution is used. The mapping (5.10) is used, because for fixed q_4, the integration of (5.1) over q gives a logarithmic singularity in q_4. This is smoothed out by (5.10).

We have tried various meshes and found that the following one gives very accurate results.

q-integration: Gaussian integration with 8 points from 0 to $2\hat{p}$ and 8 points from $2\hat{p}$ to ∞. $C_p = 2$.

q_4-integration: Gaussian integration with 12 points and $C_{p_4} = 2$.

In the single integral we have used an 8-point Gaussian integration.

6. Results

In this work it is our main intention to investigate what corrections the BSE will introduce for the $J = 0$ NN phase shifts compared to the BBS approach. The BBS couples only positive energy states [7]. The discontinuity of S_{++} (see eq. (2.11)) is given by

$$\mathrm{Disc}(S_{++}) = -\pi^2 \delta(q_0)\, \delta(E - E(q))\,, \tag{6.1}$$

from which the two-nucleon propagator is obtained via a dispersion relation [18]. The BBS finally reads

$$\phi(p) = G(p,0,1;\hat{p},0,1) + \frac{1}{\pi} \int_0^\infty \mathrm{d}q\, G(p,0,1;q,0,1) S(q)\, \phi(q)\,, \tag{6.2}$$

with

$$S(q) = \frac{1}{2} \frac{1}{E(q) - E}\,, \tag{6.3}$$

and $G(p,0,1;q,0,1)$ taken from the appendix.

Figs. 3 and 4 show the results obtained by means of the BBS for the $^1S_0$ and $^3P_0$ partial waves (dashed lines). The same exchanged particles with the same parametrization as in ref. [7] have been used. The experimental points are taken from ref. [19]. The authors of ref. [7] did not, however, take into account the term $k^\mu k^\nu/\mu_B^2$ in the propagator of the vector particles. This term is not negligible as is demonstrated in fig. 3 (dot-dashed line) for the $^1S_0$ wave, where all other parameters are the same. As we want to take into account the above term in the kernel of the BSE we have

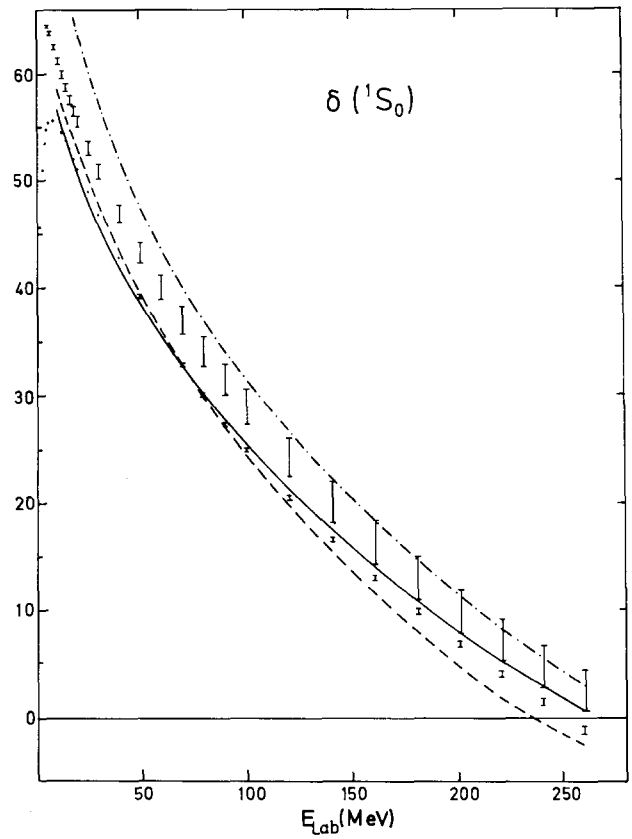

Fig. 3. Results for the $^1S_0$ phase shift. The dashed line represents the original calculation of ref. [7] in terms of the BBS. The dot-dashed line demonstrates the correction due to the term $k^\mu k^\nu/\mu_B^2$ in the propagator of the vector particles. The solid line finally shows our result obtained from the BSE with the coupling constants of table 1 ($g^2_{\omega NN}/4\pi = 12.5$). The experimental points are the energy-dependent solution of ref. [19] for the (p,p) phase shift (small error bars) and the combined (p,p) plus (n,p) experimental solution (large error bars), respectively.

to repeat the calculation with the BBS where it is included. In order to have still agreement with the experimental data, we choose $\Lambda^2 = 1.8$ (see (2.16)) instead of $\Lambda^2 = 2.2$ as in ref. [7]. Figs. 5 and 6 (dashed lines) show the new results from the BBS for the $^1S_0$ and $^3P_0$ partial waves, respectively. These curves clearly do not represent a least square fit to the experimental data anymore, but they are almost identical to the original results of ref. [7].

Figs. 5 and 6 do also show our results obtained from the BSE (solid lines) with the same "potential" (i.e. exchanged particles, coupling constants and formfactor) as was used above. The difference is particularly large for the $^1S_0$ wave which shows

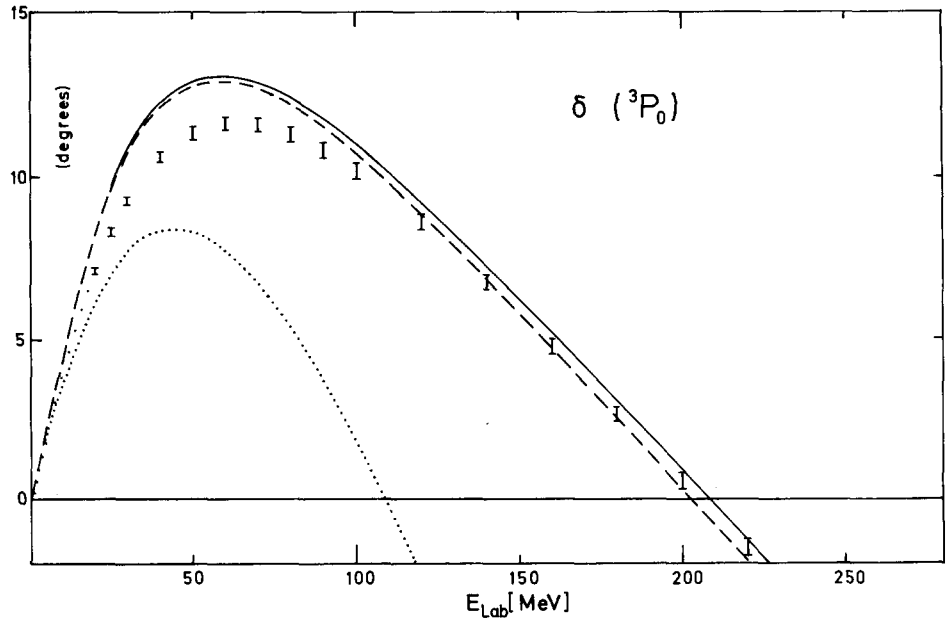

Fig. 4. Results for the $^3P_0$ phase shift. The dashed line represents the original calculation of ref. [7] in terms of the BBS. The solid line shows the result obtained from the BSE with the coupling constants of table 1 ($g^{V^2}_{\omega NN}/4\pi$ = 12.5). The dotted line is the Born term. The experimental points are the energy dependent solution of ref. [19] for the (p,p) phase shift.

considerable more attraction than the result obtained from the BBS and characteristically flattens out at higher energies. These results show that the effects from coupling between the positive and negative energy states cannot simply be neglected in describing the NN scattering as is done in the BBS equation.

The next question is if it is possible to change the coupling constants such that a reasonable description of the $J = 0$ phase shifts can be obtained in the framework of the BSE. In spite of the fact that our calculation contains a certain arbitrariness due to the introduction of the off-shell formfactor (eq. (2.16)), it seems preferable to choose coupling constants from experimental information if possible. We therefore follow Partovi and Lomon [8] in the choice of $g^{V^2}_{\rho NN}/4\pi$ and $g^{T}_{\rho NN}/g^{V}_{\rho NN}$ (see also references quoted therein). We as well accept their value for $g^2_\eta/4\pi$ which is estimated from SU(3). Beyond that it seems important in our calculation to have a larger $g^{V^2}_{\omega NN}/4\pi$ in order to properly describe the decrease of the $^1S_0$ phase shift. A large NN coupling is generally required in an off-energyshell NN-scattering theory (see ref. [13] for a comparison of various models and a compilation of the corresponding coupling constants). This effect seems to be enhanced, however, in our calculation. Fig. 3 shows the result obtained from the BSE with an $g^{V^2}_{\omega NN}/4\pi$ = 12.5

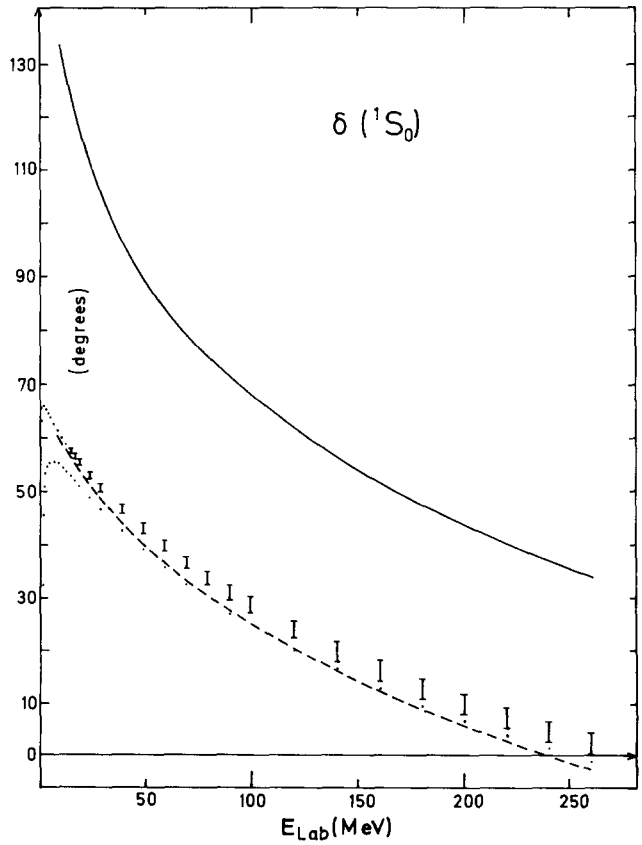

Fig. 5. Shows the comparison of the results obtained from the BBS and the BSE for the $^1S_0$ phase shift with the coupling constants of table 1 for the BBS and $\Lambda^2 = 1.8$. The experimental points are the same as in fig. 3.

and the ϵNN coupling adjusted to normalize the phase shift at $E_{lab} = 50$ MeV. Still the decrease of the phase shift obtained from the BSE (solid line) is much slower than the one obtained from the BBS (dashed line) and also is too slow compared to the experimental data.

No problems seem to occur in the description of the $^3P_0$ wave which is presented in fig. 4 (solid line). It is remarkable that we only fitted the $^1S_0$ wave by changing $g^2_{\epsilon NN}/4\pi$ and $g^{V^2}_{\omega NN}/4\pi$ and that then the $^3P_0$ phase shift agrees quantitatively almost as well with the experimental data as the least square fit performed with the BBS. Table 1 finally presents the coupling constants and particle masses which have been used in the BBS and the BSE.

It is also interesting to look at the actual convergence of the Padé approximants. Tables 2 and 3 show various orders for the $^1S_0$ and $^3P_0$ phase shifts, calculated from

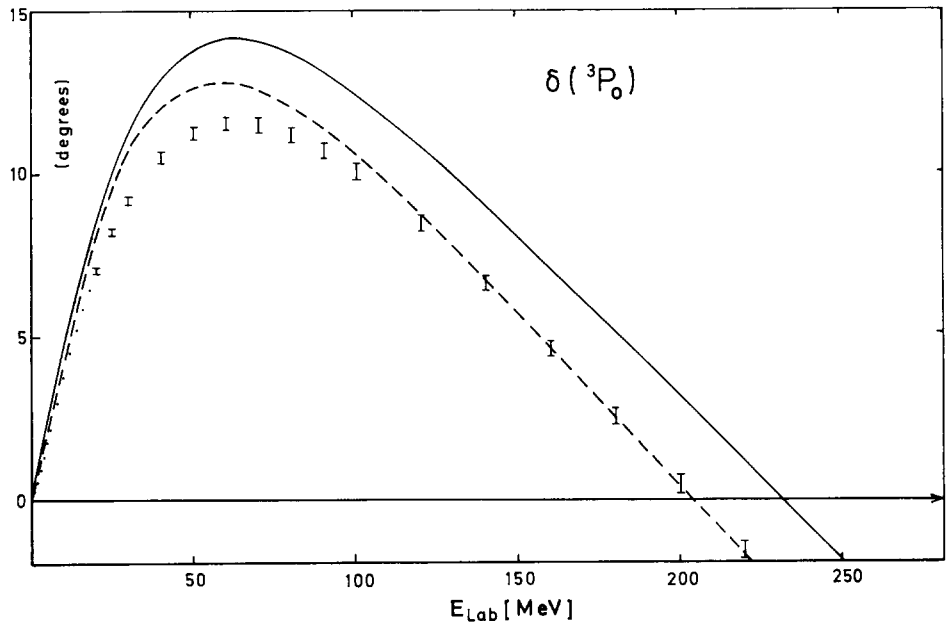

Fig. 6. Same as fig. 5 for the $^3P_0$ phase shift with the experimental points like in fig. 4.

Table 1
Masses and coupling constants used in the BBS and BSE, respectively.

		BBS	BSE
meson	m^2	$g^{(V)^2}/4\pi$	$g^{(V)^2}/4\pi$
π	0.02185	14.2	14.2
η	0.3417	3.09	1.0
ϵ	0.3691	6.97	6.2
δ	1.047	0.33	0.33
ρ	0.6613	0.43	0.53
ω	0.6961	9.92	12.5
		g^T/g^V	g^T/g^V
ρ		6.38	3.66
ω		0	0

the BSE for E_{lab} = 100 MeV. The parameters are the ones of table 1. We see that the [5/5] approximant is reasonably accurate for the $^1S_0$ phase shift, while for the $^3P_0$ wave very low orders are already extremely good. In this latter case it even makes sense to look at the Born term itself (see also ref. [20]), which is also shown in fig. 4. The born term drops down too fast, however, at higher energies.

Table 2
Padé approximants for the tg δ of the $^1S_0$ phase shift as calculated from the BSE with $g^2_{\omega NN}/4\pi = 12.5$ (see also table 1)

N	$[N/N]$	$2N$	$2N+1$
1	$-4.553 \cdot 10^{-3}$	9.14	$-4.63 \cdot 10^{1}$
2	$2.676 \cdot 10^{-1}$	$2.43 \cdot 10^{2}$	$-1.28 \cdot 10^{3}$
3	$2.151 \cdot 10^{-1}$	$6.71 \cdot 10^{3}$	$-3.52 \cdot 10^{4}$
4	$4.341 \cdot 10^{-1}$	$1.85 \cdot 10^{5}$	$-9.71 \cdot 10^{5}$
5	$4.732 \cdot 10^{-1}$	$5.10 \cdot 10^{6}$	$-2.68 \cdot 10^{7}$
6	$4.803 \cdot 10^{-1}$	$1.41 \cdot 10^{8}$	$-7.38 \cdot 10^{8}$
7	$4.806 \cdot 10^{-1}$	$3.88 \cdot 10^{9}$	$-2.04 \cdot 10^{10}$
8	$4.750 \cdot 10^{-1}$	$1.07 \cdot 10^{11}$	$-5.61 \cdot 10^{11}$
9	$4.807 \cdot 10^{-1}$	$2.95 \cdot 10^{12}$	$-1.55 \cdot 10^{13}$
10	$4.807 \cdot 10^{-1}$	$8.12 \cdot 10^{13}$	$-4.27 \cdot 10^{14}$

$E_{lab} = 100$ MeV. N is the order of the $[N/N]$ approximant. The last two columns contain the $(2N)$th and $(2N+1)$st term of the perturbation series. The numerical value of the Born term is -1.51.

Table 3
Padé approximants for the tg δ of the $^3P_0$ phase shift as calculated from the BSE with $g^2_{\omega NN}/4\pi = 12.5$ (see also table 1)

M,N	$[M/N]$	$2\max(M,N)$	$2\max(M,N)+1$
1,1	0.173 958	0.402	−0.742
1,2	0.193 410	1.51	
2.1	0.190 379	see above	
2.2	0.191 202	see above	−3.07
3,3	0.193 358	6.27	−12.8
4,4	0.193 295	26.1	−53.4
5,5–10,10 (diag.)	0.193 296	up to 10^5	

$E_{lab} = 100$ MeV. Because of the rapid convergence we have also shown the [1/2] and [2/1] approximants. M and N stand for the order of the $[M/N]$ approximants. The last two columns do again contain the corresponding terms of the power series. The numerical value of the Born term is +0.0326. The diagonal [5/5] –[10/10] approximants agree up to six decimals!

It is clear that the limiting value of the Padé sequence as shown in tables 1 and 2 is still slightly dependent on the chosen mesh (see sect. 5). The agreement of the [5/5] –[10/10] approximants for the $^3P_0$ within six decimals, e.g., does not mean that we have solved the equation to that accuracy. The rate of convergence, however, will not be very sensitive to the mesh once it is chosen properly.

It seems adequate to stress again the importance of the Padé method. If one wanted to solve the BSE for NN scattering by matrix inversion, one first of all had

to apply the regularisation procedure of ref. [15]. If one would work with our mesh (sect. 5), the problem were to invert an 800 × 800 matrix. This seems an almost impossible numerical task, in particular if one wants to do it for various partial waves and energies.

Finally we want to point out some of the checks we have made in the course of our calculation. First of all our code for the BSE reproduces roughly the perturbative terms for one-pion exchange of ref. [5] and hopefully works more accurate due to our subtraction procedure. The direct box graph agrees in this case with results obtained from dispersion relations [21] within 5 p.p.th. As a check of the kernel serves first of all the reproduction of the results obtained from the BBS. This checks the (1,1) elements of our kernels on the energy shell but off the mass shell. Furthermore we have compared the analytic expressions for the (1,1) elements of the kernel with results obtained by Perring and Phillips [22], who give a compilation of completely on shell Born terms. Last not least the REDUCE code for the analytic calculation of the kernels has been checked by comparing the results for PS, S and "photon" exchange and the crossed box graph with a hand calculation.

7. Concluding remarks

We have solved the BSE for the $J = 0$ phase shifts by applying the Padé method of summing the perturbation series. We find

(i) the phase shifts calculated from the BSE show more attraction that the ones from the BBS. The additional attraction is of the order of 50° for the $^1S_0$ wave and 2° for the $^3P_0$.

(ii) it is possible to find a fair description of the $^1S_0$ phase shift at the price of introducing a large ωNN coupling. In particular the repulsion at higher energies (~ 200 MeV) seems to be underestimated in our one-boson exchange model.

(iii) we have only fitted the $^1S_0$ wave and obtained at the same time an essential improvement of the $^3P_0$ phase shift.

As a consequence of the above results one may hope that in general the other partial waves will agree reasonably well using the BSE equation with the coupling parameters of table 1. In order to examine this, an integral equation with eight coupled channels should be solved. Again using the Padé method this is in practice possible

One of us (J.F.) is grateful to the Deutsche Forschungsgemeinschaft for financial support.

Appendix

In this appendix we present the kernels for the vertex operators (2.4), (2.5) and

(2.7). The angle integration yields the Legendre functions of second kind

$$Q_l(z) = \frac{1}{2} \int_{-1}^{+1} \frac{P_l(\cos\theta)}{z - \cos\theta} \, d(\cos\theta), \tag{A.1}$$

with the argument

$$z = \frac{p^2 + q^2 + \mu_B^2 - (p_0 - q_0)^2}{2pq} \quad . \tag{A.2}$$

The elements listed in the following stand for

$$2E(p)\,E(q)\,G(p,p_0,\alpha;\,q,q_0,\beta) \tag{A.3}$$

with the corresponding $g^2/4\pi$ put equal to 1 (also the nucleon mass $m = 1$). The general properties discussed in sect. 2 will be taken into account so that in each case only six elements need to be given.

For vertex operators which can simply be expressed as product of two operators corresponding to particle 1 and 2, respectively, one merely has to exchange Q_0 and Q_1 in order to obtain the $^3P_0$ from the $^1S_0$ kernels. This is not so in general: for $\gamma_\mu^{(1)}\,\gamma^{\mu(2)}$ ($\mu = 0,1,2,3$) e.g., the above rule applies for each term in the sum separately, but with opposite sign for $\mu = 1$ and 2. This connection can be understood from the helicity formalism: for $J = 0$ only two helicity amplitudes contribute which add like

$$\cos^2 \tfrac{1}{2}\theta \pm \sin^2 \tfrac{1}{2}\theta = \begin{cases} 1 \\ \cos\theta \end{cases} . \tag{A.4}$$

The transition from $^1S_0$ to $^3P_0$ means changing the sign of one of them. For the different kernels we finally have:

(i) Pseudosclar exchange

$^1S_0$:

$$(1,1) = -(E(p)\,E(q) - 1)\,Q_0 + pqQ_1 \,, \qquad (1,2) = -(E(p)\,E(q) + 1)\,Q_0 - pqQ_1 \,,$$

$$(1,3) = -\sqrt{2}\,(qQ_0 - pQ_1)\,, \qquad (1,4) = 0\,,$$

$$(3,3) = 2(pqQ_0 + Q_1)\,, \qquad (4,4) = -2E(p)\,E(q)\,Q_1 \,. \tag{A.5}$$

The $^3P_0$ kernel is obtained by exchanging Q_0 and Q_1.

(ii) Scalar exchange

$^1S_0$:

$$(1,1) = (E(p)\,E(q) + 1)\,Q_0 - pqQ_1 \,, \qquad (1,2) = (E(p)\,E(q) - 1)\,Q_0 + pqQ_1 \,,$$

$$(1,3) = -\sqrt{2}\,(qQ_0 + pQ_1)\,, \qquad (1,4) = 0\,,$$

$$(3,3) = 2(pqQ_0 - Q_1)\,, \qquad (4,4) = -2E(p)\,E(q)\,Q_1 \,. \tag{A.6}$$

Again the $^3P_0$ kernel is obtained by exchanging Q_0 and Q_1.

(iii) Vector exchange

It will be useful to introduce the following abbreviations

$$E_1 = E(p)^2 - E(q)^2 - k_0^2 , \qquad E_2 = E(p)^2 - E(q)^2 + k_0^2 ,$$

$$E_3 = -(E(p) - E(q))^2 + k_0^2 , \qquad E_4 = -(E(p) + E(q))^2 + k_0^2 ,$$

$$E_5 = p^2 + q^2 + k_0^2 , \qquad E_6 = p^2 + q^2 - k_0^2 . \tag{A.7}$$

We consider the vector coupling, tensor coupling and mixed terms separately.

A. Vector coupling, consisting of two terms

(a) $-\gamma_\mu^{(1)} \cdot \gamma_\mu^{(2)}$ ("photon-coupling")

$^1S_0$:

$$(1,1) = -2(2E(p)\,E(q) - 1)\,Q_0 , \qquad (1,2) = -2(2E(p)\,E(q) + 1)\,Q_0 ,$$

$$(1,3) = -2\sqrt{2}\,q\,Q_0 , \qquad (1,4) = 0 ,$$

$$(3,3) = 4pq\,Q_0 , \qquad (4,4) = -4E(p)\,E(q)\,Q_1 . \tag{A.8}$$

As described above, the $^3P_0$ matrix is not obtained by just exchanging Q_0 and Q_1. We have:

$^3P_0$:

$$(1,1) = -2(2pqQ_0 + Q_1) , \qquad (1,2) = 2(2pqQ_0 + Q_1) ,$$

$$(1,3) = -2\sqrt{2}\,(2pQ_0 - qQ_1) , \qquad (1,4) = 0 ,$$

$$(3,3) = -4(2Q_0 + pqQ_1) , \qquad (4,4) = 4E(p)\,E(q)\,Q_0 . \tag{A.9}$$

(b) $\vec{k}^{(1)} \cdot \vec{k}^{(2)}$

$^1S_0$:

$$(1,1) = ((E(p)\,E(q) + 1)\,Q_0 + pqQ_1)\,E_3 ,$$

$$(1,2) = ((E(p)\,E(q) - 1)\,Q_0 - pqQ_1)\,E_4 ,$$

$$(1,3) = \sqrt{2}\,(qQ_0 - pQ_1)\,E_1 ,$$

$$(1,4) = -2\sqrt{2}\,(qQ_0 - pQ_1)\,E(q)\,k_0 ,$$

$$(3,3) = 2((2 + E_5)\,pqQ_0 - (2p^2q^2 + E_6)\,Q_1) ,$$

$$(4,4) = -\,2E(p)\,E(q)(2pqQ_0 - E_5 Q_1) . \tag{A.10}$$

The $^3P_0$ kernel is obtained by exchanging Q_0 and Q_1.

B. Tensor coupling

$^1S_0$: we introduce the following abbreviations

$$x_1 = -9E(p)\,E(q)(E_6 Q_0 - 2pqQ_1)/12\,, \tag{A.11}$$

$$x_2 = -((3(p^2+q^2) - 2p^2q^2 + 9k_0^2)\,Q_0 + pq(3(E_6-2)\,Q_1 - 4pqQ_2))/12\,,$$

and have

$$(1,1) = x_1 + x_2\,,$$

$$(1,2) = x_1 - x_2\,,$$

$$(1,3) = \sqrt{2}\,(q(5p^2+3q^2+9k_0^2)\,Q_0 - p(3(2q^2+E_6)\,Q_1 - 4pqQ_2))/12\,,$$

$$(1,4) = \sqrt{2}\,(qQ_0 - pQ_1)\,E(q)\,k_0\,,$$

$$(3,3) = (pq(2-3(p^2+q^2) - 9k_0^2)\,Q_0 + 3(2p^2q^2 - E_6)\,Q_1 + 4pqQ_2)/6\,,$$

$$(4,4) = E(p)\,E(q)(14pqQ_0 - 3(3(p^2+q^2)+k_0^2)\,Q_1 + 4pqQ_2)/6\,. \tag{A.12}$$

Similarly for the
$^3P_0$: we introduce

$$y_1 = -E(p)\,E(q)(2pqQ_0 - 3E_6 Q_1 + 4pqQ_2)/12\,,$$

$$y_2 = -(pq(14-9E_6)\,Q_0 + 3(6p^2q^2 - 3(p^2+q^2) - k_0^2)\,Q_1 + 4pqQ_2)/12\,, \tag{A.13}$$

and have

$$(1,1) = y_1 + y_2\,,$$

$$(1,2) = y_1 - y_2\,,$$

$$(1,3) = \sqrt{2}\,(p(14q^2+9E_6)\,Q_0 - q(3(6p^2+3(p^2+q^2)+k_0^2)\,Q_1 - 4pqQ_2))/12\,,$$

$$(1,4) = \sqrt{2}\,(pQ_0 - qQ_1)\,E(q)\,k_0\,,$$

$$(3,3) = -((14p^2q^2 - 9E_6)\,Q_0 + 3pq(6-3(p^2+q^2) - k_0^2)\,Q_1 + 4p^2q^2Q_2)/6\,,$$

$$(4,4) = E(p)\,E(q)((p^2+q^2+3k_0^2)\,Q_0 - 2pqQ_1)/2\,. \tag{A.14}$$

C. Mixed coupling

In this case there is no term proportional $E(q)$ in the upper l.h. 2×2 matrix. Therefore we just have $(1,2) = -(1,1)$. Similarly $(4,4) = 0$. This is true for both partial waves.

The remaining elements are, for the
$^1S_0$:

$$(1,1) = -(p^2+q^2)Q_0 + 2pqQ_1 \,, \qquad (1,3) = -\sqrt{2}\,(q(1-p^2)Q_0 - p(1-q^2)Q_1)\,,$$

$$(1,4) = -\sqrt{2}\,pE(q)\,k_0 Q_1 \,, \qquad (3,3) = 2(2pqQ_0 - (p^2+q^2)Q_1)\,, \qquad \text{(A.15)}$$

and
$^3P_0$:

$$(1,1) = -3(2pqQ_0 - (p^2+q^2)Q_1)\,, \qquad (1,3) = -3\sqrt{2}\,(p(1-q^2)Q_0 - q(1-p^2)Q_1)\,,$$

$$(1,4) = 3\sqrt{2}\,pE(q)\,k_0 Q_0 \,, \qquad (3,3) = 6((p^2+q^2)Q_0 - 2pqQ_1)\,. \qquad \text{(A.16)}$$

These differ from the above only by a factor -3 and the exchange of Q_0 and Q_1.

References

[1] J.L. Gammel and R.M. Thalor, Phys. Rev. 107 (1957) 291, 1337; Progress in elementary particle and cosmic ray physics V (North-Holland, Amsterdam, 1960) p. 99.
[2] T. Hamada and I.D. Johnston, Nucl. Phys. 34 (1962) 382.
[3] M. Fortes and A.D. Jackson, Nucl. Phys. A175 (1971) 449.
[4] T. Murota, M.-T. Noda and F. Tanaka, Progr. Theor. Phys. (Kyoto) 46 (1971) 1456; H. Ito, T. Murota, M. Noda and F. Tanaka, Progr. Theor. Phys. 51 (1974) 1115.
[5] J.L. Gammel, M.T. Menzel and W.R. Wortman, Phys. Rev. D3 (1971) 2175; J.L. Gammel and M.T. Menzel, Phys. Rev. D7 (1973) 565.
[6] G. Schierholz, Nucl. Phys. B40 (1972) 335.
[7] A. Gersten, R.H. Thompson and A.E.S. Green, Phys. Rev. D3 (1971) 2076.
[8] M.H. Partovi and E.L. Lomon, Phys. Rev. D2 (1970) 1999.
[9] J.J. Kubis, Phys. Rev. D6 (1972) 547.
[10] M.L. Goldberger, M.T. Grisaru, S.W. MacDowell and D.Y. Wong, Phys. Rev. 120 (1960) 2250.
[11] J. Fleischer, J. Comp. Phys. 12 (1973) 112.
[12] A.C. Hearn, REDUCE 2 User's Manual, Stanford Artificial Intelligence Project, MEMO AIM-133, October 1970.
[13] H. Pilkuhn et al., Nucl. Phys. B65 (1973) 460.
[14] S. Mandelstam, Proc. Roy. Soc. A237 (1956) 496.
[15] M. Levine, J. Tjon and J. Wright, Phys. Rev. Letters 16 (1966) 962.
[16] J.S.R. Chisholm, J. Math. Phys. 4 (1963) 1506.
[17] J. Nuttall, J. Math. Anal. and Appl. 31 (1970) 147; G.A. Baker, jr., BNL-preprint.
[18] R. Blankenbecler and R. Sugar, Phys. Rev. 142 (1966) 1051.
[19] M.H. McGregor, R.A. Arndt and R.M. Wright, Phys. Rev. 182 (1969) 1714.
[20] J. Binstock and R. Bryan, Phys. Rev. D4 (1971) 1341.
[21] W.R. Wortman, Private communication; D. Bessis, G. Turchetti and W.R. Wortman, Phys. Rev. Letters 39B (1972) 601.
[22] J.K. Perring and R.J.N. Phillips, AERE-R. 4077 (June 1962) unpublished.